Bioorganic & Medicinal Chemistry Letters 21 (2011) 1582–1587

Contents lists available at ScienceDirect

Bioorganic & Medicinal Chemistry Letters

journal homepage: www.elsevier.com/locate/bmcl

Structure and property based design of factor Xa inhibitors: Pyrrolidin-2-ones with aminoindane and phenylpyrrolidine P4 motifs

Robert J. Young [a,*], Carl Adams [a], Mike Blows [a], David Brown [a], Cynthia L. Burns-Kurtis [b], Chuen Chan [a], Laiq Chaudry [a], Máire A. Convery [a], David E. Davies [a], Anne M. Exall [a], Graham Foster [a], John D. Harling [a], Eric Hortense [a], Stephanie Irvine [a], Wendy R. Irving [a], Steve Jackson [a], Savvas Kleanthous [a], Anthony J. Pateman [a], Angela N. Patikis [a], Theresa J. Roethka [b], Stefan Senger [a], Gary J. Stelman [b], John R. Toomey [b], Robert I. West [a], Caroline Whittaker [a], Ping Zhou [a], Nigel S. Watson [a]

[a] GlaxoSmithKline, Medicines Research Centre, Gunnels Wood Road, Stevenage, Hertfordshire SG1 2NY, United Kingdom
[b] GlaxoSmithKline, 709 Swedeland Road, King of Prussia, PA 19406, USA

ARTICLE INFO

Article history:
Received 17 December 2010
Revised 26 January 2011
Accepted 27 January 2011
Available online 1 February 2011

Keywords:
Factor Xa
Oral inhibitors
Property based design
Structure based design
P450 inhibition

ABSTRACT

The rational design, syntheses and evaluation of potent sulfonamidopyrrolidin-2-one-based factor Xa inhibitors incorporating aminoindane and phenylpyrrolidine P4 motifs are described. These series delivered highly potent anticoagulant compounds with excellent oral pharmacokinetic profiles; however, significant time dependant P450 inhibition was an issue for the aminoindane series, but this was not observed with the phenylpyrrolidine motif, which produced candidate quality molecules with potential for once-daily oral dosing in humans.

© 2011 Elsevier Ltd. All rights reserved.

The approvals for the selective thrombin inhibitor dabigatran[1] and factor Xa (fXa) inhibitor rivaroxaban,[2] were significant milestones in the search for new, small molecule, treatments for thrombosis, through targeting single protease enzymes in the blood coagulation cascade. These selective medicines do not require extensive monitoring due to their reduced bleeding liability compared with established agents such as the coumarins.[3] This highly competitive field has seen many selective inhibitors of the

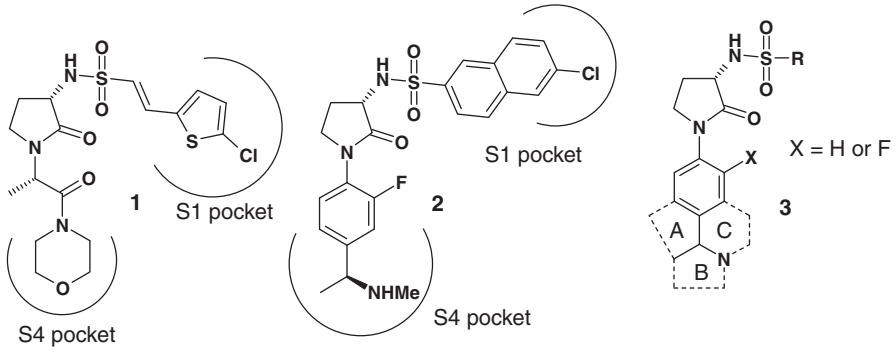

Figure 1. Clinical candidate **1**, αMBA **2** and generic constrained structures **3**.

* Corresponding author. Tel.: +44 1438 768372.
E-mail address: Rob.J.Young@gsk.com (R.J. Young).

0960-894X/$ - see front matter © 2011 Elsevier Ltd. All rights reserved.
doi:10.1016/j.bmcl.2011.01.131

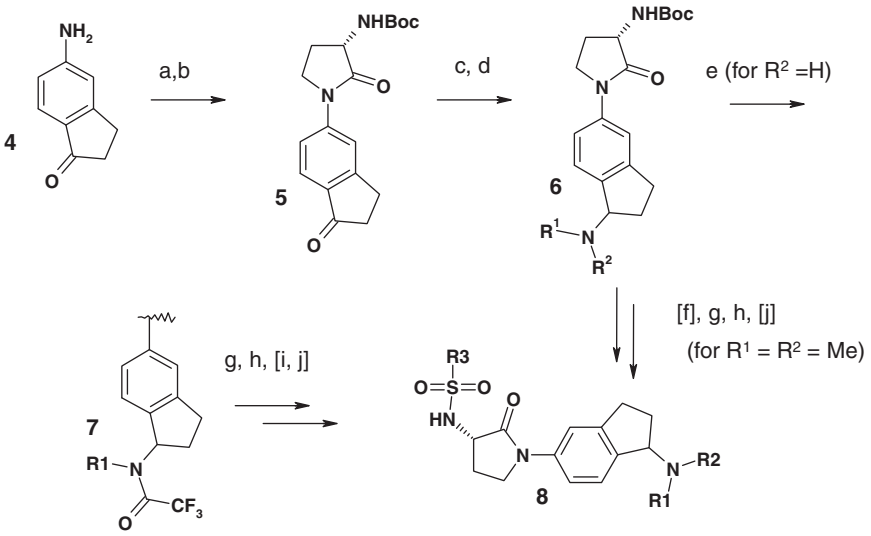

Scheme 1. Reagents and conditions: (a) Boc-Met-OH, HATU, DIPEA, DCM, rt 95%; (b) MeI, MeCN, rt, then Cs_2CO_3, MeCN, 60 °C, 67%; (c) $NaBH_4$, MeOH, rt, 95%; (d) $MeSO_2Cl$, Et_3N, DCM, −76 °C; then R^1R^2NH, THF, rt, 40%; (e) TFAA, DCM, rt, 62%; [(f) chiral hplc]; (g) HCl, MeOH, rt, 95%; (h) R^3SO_2Cl, pyridine, MeCN, rt, 60–90%, (i) Na_2CO_3, aq MeOH, rt, 45%; (j) for *N*-TIPS-protected indole-P1; Et_4NF, THF, rt, 90%.

trypsin-like serine proteases thrombin and fXa progress to the clinic and further trials continue.[2c,3f]

Our programme of work on fXa inhibitors has focussed on the sulfonamidopyrrolidin-2-one template, exemplified by our first clinical candidate **1**,[4] featuring the morpholine alanyl amide P4 ligand (Fig. 1). The structurally similar S1 binding pockets of thrombin and fXa normally bind a basic amino acid, forming a salt bridge with asparate189; however, chloroaromatics have been used to exploit binding to tyrosine228 in our fXa series[4,5] and, for example, in rivaroxaban.[2] This enabled the discovery of neutral compounds with enhanced oral bioavailability over earlier basic inhibitors.[3] Whilst SAR studies[4a] for ligands binding in the S1 pocket have shown limited scope for variations that maintain potency, plasma-based activity and good DMPK properties, the back-up programme identified a number of novel P4 motifs (replacing the morpholine alanyl amide of **1**, with the aim of improving pharmacokinetic half-life) through the exploitation of structure-based design.[5] Through strict attention to molecular properties, acceptable levels of oral pharmacokinetic exposure were achieved with these combinations, whereby moderately basic P4 groups were exploited to modulate hydrophobicity. However, time-dependent inhibition (TDI) of Cyp3A4 curtailed the progress of the recently disclosed α-methyl benzylamine (αMBA) series,[5c] exemplified by **2**. Growth and fusion of the benzylic amine motif into a cyclic structure represented an attractive strategic extension; three such constrained series are generically represented as **3** A, B and C in Figure 1. Aminoindanes and phenylpyrrolidines, represented by A and B, respectively, are described herein; the tetrahydroisoquinolines and related structures denoted by C are described in the accompanying paper.

Computational docking studies using FLO[6] indicated that each of these structures was likely to maintain good contacts in the S4 pocket. Docking studies also provided the impetus to synthesise 6-indolylsulfonyl P1 analogues,[7] which were predicted to maintain

Table 1
fXa inhibitory activities,[15] anticoagulant potency[16] and physical descriptors[17] for compounds **1**, **2** and **9–17**, with P1 structures and abbreviations

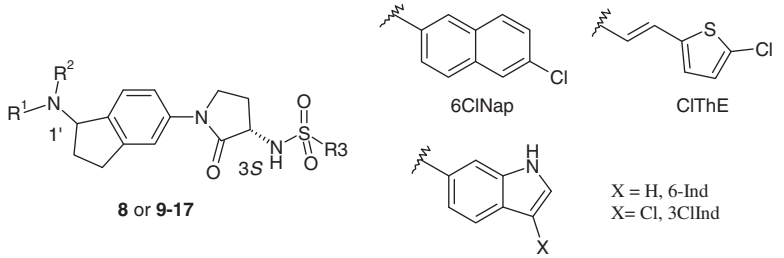

Entry	R^3	1′ Stereo	R^1	R^2	FXa (K_i, nM)	1.5 × PT (μM)	*c* log $D_{7.4}$	MW	cmr
1	ClThE	Ala-morpholine			4	1.2	2.7	447	10.9
2	6ClNap	*R*	Me	H	2	7.0	1.6	476	12.5
9	ClThE	*R/S*	Me	Me	4	1.4	2.0	466	12.3
10	6ClNap	*R/S*	Me	Me	3	4.7	2.2	484	13.2
11	6ClNap	*S*	Me	Me	2	3.9	2.2	484	13.2
12	6ClNap	*R*	Me	Me	9	7.4	2.2	484	13.2
13	3ClInd	*R/S*	Me	Me	1	0.9	1.9	473	12.6
14	ClThE	*R/S*	Me	H	4	2.6	0.9	452	11.8
15	6ClNap	*R/S*	Me	H	5	6.5	1.2	470	12.7
16	3ClInd	*R/S*	Me	H	0.3	2.8	0.1	440	12.6
17	6ClNap	*R/S*	H	H	5	13.3	0.9	456	12.3

Table 2
Rat DMPK parameters[18] for **2** and aminoindanes **9, 11, 12, 14** and **15**

Entry	Me_n	Stereo-chem	Cl_p[a] (mL/min/kg)	$T_{1/2}$[b] (h)	V_{ss}[c] (L/kg)	F[d] (%)
2	1	*R*	1.6	18	2.4	>10
9	2	*R/S*	9.5	1.7	1.1	57
11	2	*S*	6	4.4	2.0	61
12	2	*R*	7.6	3.4	1.7	27
14	1	*R/S*	2.2	5.4	0.9	nd
15	1	*R/S*	2.5	12.4	2.4	25

[a] Cl_p, plasma clearance expressed as mL/min/kg.
[b] $T_{1/2}$, half-life of the test compound expressed in h.
[c] V_{ss}, steady state volume of distribution expressed as L/kg.
[d] *F*, oral bioavailability expressed as %.

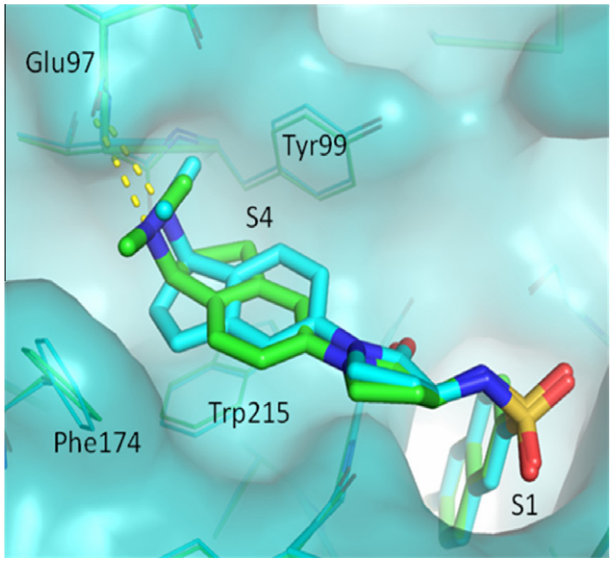

Figure 2. Overlay of observed binding modes of **11** (green) and **12** (cyan) showing contacts in the fXa S4 pocket: hydrogen bonds to Glu97 and proximity of Tyr99, Phe174 and Trp215.

good physical properties and overlaid effectively with alternative P1 structures in the sulfonamidopyrrolidin-2-one series[4a] and other inhibitors exploiting indolyl P1 motifs.[8] Importantly, the P4 targets offered potential alternative routes of metabolism (via, for example, conjugation into indene, pyrrolene or dihydroquinoline ring systems) which might address the TDI seen in the αMBA series, which has been postulated to arise through the generation of a reactive nitroso metabolite.[9] With these modest structural modifications, the desirable size (expressed as calculated molar refraction, cmr) and hydrophobicity characteristics achieved with **2** would be maintained,[5c] while enhancing conformational restraint. Such properties were expected to facilitate the attainment of good pharmacokinetic profiles and efficient translation of anticipated fXa potency into good levels of anticoagulant activity. The latter was anticipated due to expected modest levels of plasma protein binding, with favourable binding kinetics,[10] of relatively hydrophilic compounds with only 2 or 3 aromatic rings.[11]

Targets in the aminoindane series were synthesised via homochiral pyrrolidin-2-one ring construction (Scheme 1) using established chemistry from commercial 5-amino indanone **4** and *N*-Boc methionine.[12] The amino functionality was introduced (as an epimeric mixture) by reduction of the ketone **5** to the corresponding alcohol, mesylation and displacement by either ammonia, methylamine or dimethylamine. These intermediates **6** were *N*-protected as the trifluoroacetamide **7** in the amino (**6**, $R^1 = R^2 = H$) or methylamino examples (**6**, $R^1 = H$, $R^2 = Me$). Acidic deprotection of the 3-*N*-Boc group and sulfonylation furnished the final *N,N*-dimethylamino ($R^1 = R^2 = Me$) analogues **8**; trifluoroacetamide protection was removed using sodium carbonate in aqueous methanol to furnish the other variants of **8**. The indolyl sulphonyl chlorides[13] were *N*-triisopropylsilyl (TIPS) protected, thus an additional fluoride deprotection step was required to furnish these P1 analogues. To access homochiral compounds, the diastereomers of dimethylamino intermediate **6** were separated by preparative chiral HPLC,[14] and then processed in the same manner as the racemate.

The fXa potencies[15] achieved in the aminoindane series were at least comparable to the αMBA series, exemplified by **2**, which translated into useful levels of anticoagulant activity[16] as expected from the predicted physical properties[17] (Table 1). These data were complemented by encouraging rat pharmacokinetics (Table 2),[18] with trends and values similar to the αMBA series; the *N*-monomethyl analogues again displayed extended half-lives in comparison to the *N,N*-dimethyl compounds. Particularly encouraging activity data were secured with the 3-chloroindol-6-yl derivates **13** and **16**. However, full evaluation of this aminoindane P4 motif was curtailed by Cyp3A4 studies with **10**, **15** and **17**.[19] Whilst the levels of TDI observed were lower than those observed in the αMBA series, they remained significant. As this series retained a pendant amino group, it was postulated that metabolism of the nitrogen via a likely nitroso species, as proposed for the αMBA series,[5c] was the most relevant path, rather than elimination via an indene.

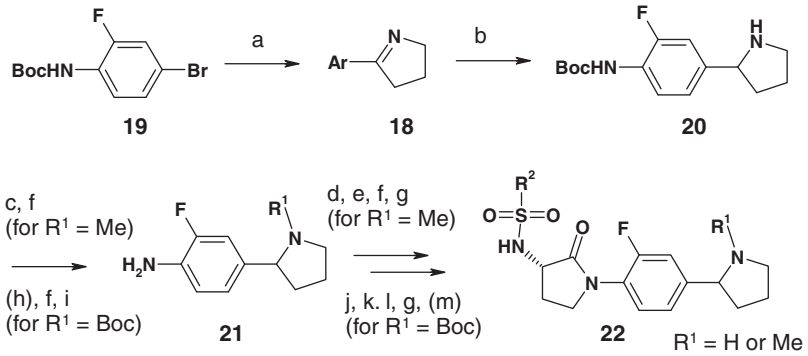

Scheme 2. Reagents and conditions: (a) *n*BuLi, pyrrolidinone-OTMS, THF, −78 °C to rt, 60%; (b) $NaBH_4$, MeOH, rt, 90%; (c) HCO_2H, $H_2C{=}O$, $CHCl_3$, reflux, 95%; (d) *N*-Boc homoserine lactone, Me_3Al, DCM, 0 °C to rt; (e) DtBAD, Bu_3P, THF, rt, 49% (d and e); (f) HCl, MeOH, rt, 95%; (g) R^2SO_2Cl, pyridine, MeCN, rt, 75–95%; (h) optional chiral hplc; (i) Boc_2O, DCM, rt, 90%; (j) Cbz-Met-OH, HATU, DIPEA, DCM, rt, 95%; (k) MeI, MeCN, 60 °C, then Cs_2CO_3, 79%; (l) H_2, $Pd(OH)_2$–C, EtOH, rt, quant.; (m) optional for *N*-TIPS-protected indole-P1; Et_4NF, THF, rt, 90%.

Table 3
fXa inhibitory activities,[15] anticoagulant potency[16] and physical descriptors[17] for compounds **23–32**

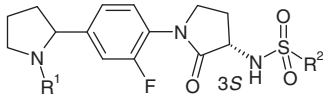

22 or **23-32**

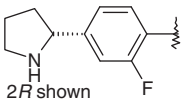

Entry	R^2	Stereo	R^1	FXa (K_i, nM)	1.5 × PT (μM)	*c* log $D_{7.4}$	MW	cmr
23	ClThE	*R/S*	Me	15	1.6	0.9	484	12.3
24	6ClNap	*R/S*	Me	6	8.6	1.1	502	13.2
25	ClThE	*R/S*	H	5	3.2	1.1	470	11.9
26	6ClNap	*R/S*	H	2	8.0	1.4	488	12.8
27	3ClInd	*R/S*	H	2	2.9	1	477	12.2
28	6-Ind	*R/S*	H	100	9.9	0.1	442	11.7
29	ClThE	*R*	H	3	0.7	1.1	470	11.9
30	ClThE	*S*	H	6	1.8	1.1	470	11.9
31	6ClNap	*R*	H	2	4.5	1.4	488	12.8
32	6ClNap	*S*	H	4	7.7	1.4	488	12.8

Table 4
Rat DMPK parameters[18] for phenylpyrrolidines

	P1	Stereochem	R^2	Cl_p[a] (ml/min/kg)	$T_{1/2}$[b] (h)	V_{ss}[c] (L/kg)	F[d] (%)
23	ClThE	*R/S*	Me	11	1.4	0.8	41
25	ClThE	*R/S*	H	2.8	3.4	0.7	52
27	3ClInd	*R/S*	H	1.3	11	0.8	<1
26	6ClNap	*R/S*	H	2.7	9.0	1.9	24
31	6ClNap	*R*	H	2.6	10.2	1.9	25
32	6ClNap	*S*	H	2.8	7.5	1.7	38

[a–d] As Table 2.

Effective binding, leading to maintenance of fXa activity was predicted by modelling for each of the 1′-epimeric pair of indanes **11** and **12**. This was substantiated by X-ray crystal structures of **11** and **12** bound into fXa; the whole indane rotates through 180° to maintain the contact between the terminal amine and the backbone carbonyl of Glu97, with each of these maintaining stacking and edge on hydrophobic contacts with the box resides Tyr99, Phe174 and Trp215 (Fig. 2).[20]

The key bond forming reaction towards the 2-phenylpyrrolidine series was construction of pyrroline **18** by reaction of lithiated *N*-Boc-2-fluoro-4-bromoaniline **19** with TMS pyrrolidinone[21] (Scheme 2). Following sodium borohydride reduction, Eschweiler–Clarke N-methylation of **20**, followed by acidic deprotection gave an intermediate (**21**, R^1 = Me) for pyrrolidinone construction using *N*-Boc-homoserine lactone and trimethylaluminium methodology;[22] this was progressed towards targets **22** as described in Scheme 1. The activity of these compounds provided an impetus to design a route to access the des-methyl analogues; moreover preparative chiral hplc of pyrrolidine **20** facilitated access its homochiral enantiomers in multi-gram quantities.[23] Subsequently, the position of *N*-Boc protection was switched by deprotection of homochiral (or racemic) **20** under acidic conditions and selective reaction of the more basic aliphatic nitrogen with Boc anhydride, furnishing **21**, R^1 = Boc. These intermediates were converted into homochiral des-methyl target compounds **22** exploiting construction of the pyrrolidinone from Cbz-methionine and elaboration as described in Scheme 1.[24]

The fXa potencies achieved with *N*-methyl **23** and **24** translated into useful anticoagulant activity (Table 3), which, combined with encouraging oral exposure for **23** (Table 4) provided the impetus to pursue the series further. In the des-methyl series, low nM potency was achieved in molecules with similar anticoagulant activities and longer pharmacokinetic half-lives, again driven by lower clearance associated with this tertiary to secondary amine modification (vide supra). Good oral bioavailability was achieved with (*E*)-2-(5-chlorothien-2-yl)ethenyl (ClThE) **25** and 6-chloronaphth-2-yl (6ClNap) **26** motifs, however the otherwise attractive profile of the 3-chloroindol-6-yl **27** was undermined by the lack of oral exposure. The *R*-ClThE **29** was one of the most potent anticoagulants with the sulfonamidopyrrolidin-2-one template, whilst *R*-6-Chloronaphth-2-yl **31** showed the potential for once daily dosing based on the rat studies. No selectivity issues were apparent against our panel of trypsin-like serine proteases[25] and, more significantly, the risk of time dependant inhibition of Cyp3A4 was

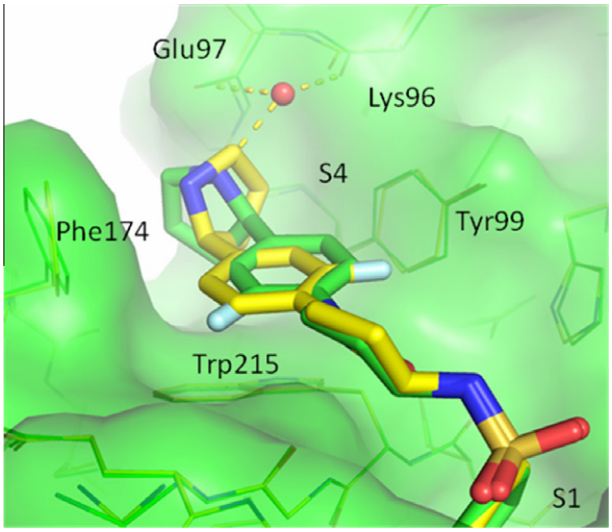

Figure 3. Overlay of the X-ray crystal structures of **31** (green) and **32** (yellow) showing contacts in the fXa S4 pocket: water mediated hydrogen bonding to Lys 96/Glu97 with **31** and proximity of Tyr99, Phe174 and Trp215.

effectively discharged.[26] Taken together these data formed a package warranting further investigation of this series.

X-ray structures[27] of **31** and **32** bound into fXa showed the diastereomeric sub-units in the P4 pocket (Fig. 3). The S1 pocket is occupied by the aromatic sulfonamide group as seen throughout previously reported series.[4,5] The distal pyrrolidine ring of *S,R*-**31** makes hydrophobic contacts with the Trp215 residue though a 3.5 Å $CH_2\cdots\pi$ interaction.[28] The likely protonated ring nitrogen makes water-mediated hydrogen bonds to the backbone carbonyls of Lys96 and Glu97. In epimeric *S,S*-**32** the confirmation of the pyrrolidine ring required to allow orientation of the ring nitrogen atom towards Glu97 meant that it did not reach quite as far into the hydrophobic cleft of the pocket, whilst maintaining contacts with Trp215 through the equivalent methylene in a similar position and without the water mediated hydrogen bond from the nitrogen.

In conclusion, two approaches have been described to expand upon the SAR of fXa inhibitors incorporating the α-methyl benzylamine (αMBA) P4 motif, which were designed to constrain the molecules and to address the risk of Cyp3A4 TDI in the αMBA series. These studies have led to the discovery of potent and long-lasting oral inhibitors of fXa incorporating aminoindane and phenylpyrrolidine P4 groups. Importantly, the latter series effectively addressed the key issue of TDI and provided candidate quality molecules; these have been progressed into further studies that will be reported in due course.

References and notes

1. (a) Eikelboom, J. E.; Weitz, J. I. *Thromb. Haemost.* **2009**, *101*, 2; (b) Sanford, M.; Plosker, G. L. *Drugs* **2008**, *68*, 1699; (c) Sobera, L. A.; Bozzo, J.; Castaner, J. *Drugs Future* **2005**, *30*, 877.
2. (a) Abrams, P. J.; Emerson, C. R. *Pharmacotherapy* **2009**, *29*, 167; (b) Escolar, G.; Villalta, J.; Casals, F.; Bozzo, J.; Serradell, N.; Bolos, J. *Drugs Future* **2006**, *31*, 484; (c) Perzborn, E.; Roehrig, S.; Straub, A.; Kubitza, D.; Misselwitz, F. *Nat. Rev. Drug Disc.* **2011**, *10*, 61.
3. (a) Sobieraj-Teague, M.; O'Donnell, M.; Eikelboom, J. *Semin. Thromb. Hemost.* **2009**, *35*, 515; (b) Harenberg, J.; Wehling, M. *Semin. Thromb. Hemost.* **2008**, *34*, 39; (c) Lassen, M. R. *Expert Opin. Pharmacother.* **2009**, *10*, 1769; (d) Gomez-Outes, A.; Lecumberri, R.; Pozo, C.; Rocha, E. *Curr. Vasc. Pharmacol.* **2009**, *7*, 309; (e) Eriksson, B. I.; Quinlan, D. J.; Weitz, J. I. *Clin. Pharmacokinet.* **2009**, *48*, 1; (f) Pinto, D. J. P.; Smallheer, J. M.; Cheney, D. L.; Knabb, R. M.; Wexler, R. R. *J. Med. Chem.* **2010**, *53*, 6243.
4. (a) Chan, C.; Borthwick, A. D.; Brown, D.; Burns-Kurtis, C. L.; Campbell, M.; Chaudry, L.; Chung, C.-W.; Convery, M. A.; Hamblin, J. N.; Johnstone, L.; Kelly, H. A.; Kleanthous, S.; Patikis, A.; Patel, C.; Pateman, A. J.; Senger, S.; Shah, G. P.; Toomey, J. R.; Watson, N. S.; Weston, H. E.; Whitworth, C.; Young, R. J.; Zhou, P. *J. Med. Chem.* **2007**, *50*, 1546–1557; (b) Abboud, M. A.; Needle, S. J.; Burns-Kurtis, C. L.; Valocik, R. E.; Koster, P. F.; Amour, A. J.; Chan, C.; Brown, D.; Chaudry, L.; Zhou, P.; Patikis, A.; Patel, C.; Pateman, A. J.; Young, R. J.; Watson, N. S.; Toomey, J. R. *J. Cardiovasc. Pharmacol.* **2008**, *52*, 66.
5. (a) Young, R. J.; Borthwick, A. D.; Brown, D.; Burns-Kurtis, C. L.; Campbell, M.; Chan, C.; Charbaut, M.; Chung, C.-w.; Convery, M. A.; Kelly, H. A.; King, N. P.; Kleanthous, S.; Mason, A. M.; Pateman, A. J.; Patikis, A. N.; Pinto, I. L.; Pollard, D. R.; Senger, S.; Shah, G. P.; Toomey, J. R.; Watson, N. S.; Weston, H. E. *Bioorg. Med. Chem. Lett.* **2008**, *18*, 23; (b) Young, R. J.; Borthwick, A. D.; Brown, D.; Burns-Kurtis, C. L.; Campbell, M.; Chan, C.; Charbaut, M.; Convery, M. A.; Diallo, H.; Hortense, E.; Irving, W. R.; Kelly, H. A.; King, N. P.; Kleanthous, S.; Mason, A. M.; Pateman, A. J.; Patikis, A. N.; Pinto, I. L.; Pollard, D. R.; Senger, S.; Shah, G. P.; Toomey, J. R.; Watson, N. S.; Weston, H. E.; Zhou, P. *Bioorg. Med. Chem. Lett.* **2008**, *18*, 28; (c) Kleanthous, S.; Borthwick, A. D.; Brown, D.; Burns-Kurtis, C. L.; Campbell, M.; Chan, C.; Chaudry, L.; Clarte, M. O.; Convery, M. A.; Harling, J. D.; Hortense, E.; Irving, W. R.; Irvine, S.; Pateman, A. J.; Patikis, A. N.; Pinto, I. L.; Pollard, D. R.; Roethka, T. J.; Senger, S.; Shah, G. P.; Stelman, G. J.; Toomey, J. R.; Watson, N. S.; West, R. I.; Whittaker, C.; Zhou, P.; Young, R. J. *Bioorg. Med. Chem. Lett.* **2010**, *20*, 618.
6. QXP/FLO, ThistleSoft Inc.: Colebrook, C. T.; McMartin, C.; Bohacek, R. S. *J. Comput. Aided Mol. Des.* **1997**, *11*, 333.
7. Shi, Y.; Sitkoff, D.; Zhang, J.; Klei, H. E.; Kish, K.; Liu, E. C.-K.; Hartl, K. S.; Seiler, S. M.; Chang, M.; Huang, C.; Youssef, S.; Steinbacher, T. E.; Schumacher, W. A.; Grazier, N.; Pudzianowski, A.; Apedo, A.; Discenza, L.; Yanchunas, J.; Stein, P. D.; Atwal, K. S. *J. Med. Chem.* **2008**, *51*, 7541.
8. Franciskovicha, J. B.; Masters, J. J.; Weber, W. W.; Klimkowski, V. J.; Chouinard, M.; Sipes, P. R.; Johnson, L. M.; Snyder, D. W.; Chastain, M. K.; Craft, T. J.; Towner, R. D.; Gifford-Moore, D. S.; Froelich, L. L.; Smallwood, J. K.; Foster, R. S.; Smith, G. F.; Liebeschuetz, J. W.; Murray, C. W.; Young, S. C. *Bioorg. Med. Chem. Lett.* **2007**, *17*, 6910.
9. (a) Kalgutkar, A. S.; Gardner, I.; Obach, R. S.; Shaffer, C. L.; Callegari, E.; Henne, K. R.; Mutlib, A. E.; Dalvie, D. K.; Lee, J. S.; Nakai, Y.; O'Donnell, J. P.; Boer, J.; Harriman, S. P. *Curr. Drug Metab.* **2005**, *6*, 161; (b) Kalgutkar, A. S.; Obach, R. S.; Maurer, T. S. *Curr. Drug Metab.* **2007**, *8*, 407.
10. We have previously reported on our understanding of the role of plasma protein binding in the relationship between intrinsic factor Xa activity and anticoagulant activity; the extent of binding gives only a partial explanation, due to the multiple variables inherent in the process (see note 15 of Ref.[5a] above).
11. (a) Ritchie, T. J.; MacDonald, S. J. F. *Drug Discovery Today* **2009**, *14*, 1011; The recognition of an additive contribution of hydrophobicity plus number of aromatic rings in impacting solubility was noted in: (b) Hill, A. P.; Young, R. J. *Drug Discovery Today* **2010**, *15*, 648–655; This observation also holds for %HSA binding, to be published shortly in Young, R. J.; Green, D. V. S.; Luscombe, C. N.; Hill, A. P. *Drug Discovery Today*, **2011** invited submission, manuscript under review.
12. By analogy to our previous publications[4a,5] these transformations were expected to have produced homochirality at *N*-3; findings of chiral hplc studies[14] of final compounds were consistent with this notion.
13. Harling, J. D.; Watson, N. S.; Young, R. J. WO108709 A1, 2006.
14. An analytical separation was achieved on a Chiracel OJ column, eluted with 15% EtOH in heptanes; the isomers had retention times of 8.7 min and 11.2 min for *S,S* and *S,R*, respectively. This was scaled to a preparative column to deliver compounds **11** and **12** with ee and de of >96%.
15. Factor Xa inhibitory activities were determined using Rhodamine 110, bis-(CBZ-glycylglycyl)-L-arginine amide as the fluorogenic substrate; details are described in Ref.[4a].
16. Anticoagulant activities were determined in the prothrombin time (PT) assay; see Ref.[4a], expressed as the concentration required to extend the control coagulation time by 50% (1.5 × PT).
17. Hydrophobicity predictions, expressed as $c\log D_{7.4}$, were all re-calculated using Advanced Chemistry Development software v11.0 to ensure consistency in this paper; calculated molecular refractivity (cmr) was derived from Daylight software v4.9. The paradoxical advantage of these $c\log D_{7.4}$ predictions over actual octanol–water measurements is noted in Ref.[11b]; we have quoted these through all of our publications for consistency.
18. Pharmacokinetics measured in male Sprague–Dawley rats following intravenous and oral administration. The formulation used for both iv and po dosing was a 5:95% (v/v) mixture of DMSO and 50:50 PEG-200: sterile water. Serial blood samples were collected into heparinised containers at various time-points and blood centrifuged to yield plasma. These studies used at least three animals for each (iv/po) leg.
19. Amino indene TDI experiments were carried out at Biodynamics (www.biodynamics.co.uk) and were reported as fold shifts in the observed Cyp3A4 (BFC substrate) IC_{50} after 25 min incubation versus the initial IC_{50} value. Apparent TDI was detected for compounds **10**, **15** and **17** with 2.2, 2.5 and 2.1-fold shifts (respectively) in the IC_{50}; compared with 5.8-fold for **2** in a parallel assay.
20. The structure for **11** was refined at 1.85 Å (overall R_{merge} is 0.16) in Refmac5 to a final R_{factor} of 0.196 and R_{free} of 0.246 and **12** was refined at 1.9 Å (overall R_{merge} is 0.061) in Refmac5 to a final R_{factor} of 0.189 and R_{free} of 0.241 using procedures described in Ref.[4a]. Co-ordinates are deposited in the protein databank with codes 2y7z **11** and 2y80 **12**. These structures and many others unpublished from our factor Xa series will be made available via the Community Structure–Activity Resource at the University of Michigan (www.csardock.org).
21. Feringa, B. L.; Jansen, J. F. G. A. *Tetrahedron Lett.* **1986**, *27*, 507.
22. Bell, I. M.; Beshore, D. C.; Gallicchio, S. N.; Williams, T. M. *Tetrahedron Lett.* **2000**, *41*, 1141.
23. An analytical separation was achieved on a Chiralpak AD column, eluted with 15% EtOH in heptanes with 0.1% TFA; the isomers had retention times of 4.8 min and 6.7 min for *S* and *R*, respectively. This was scaled to a preparative column to deliver both enantiomers of **20** with ee of >96% in multi-gram quantities.
24. ^{19}F NMR of Mosher amides of the intermediate amines between **21** and **22** indicated that these transformations gave homochirality at this centre. The diastereomeric excess of final compounds **31** and **32** was shown to be >96% by chiral hplc on a Chiralpak AD column, eluted with 50% EtOH in heptanes with 0.1% TFA; the isomers had retention times of 4.6 min and 8.6 min *S,R*-**31** and *S,S*-**32**, respectively.
25. Selectivity data versus a panel of trypsin-like serine proteases, expressed as fold selectivity by ratio of K_i values.

	fIIa	tPA	Kallikrein	APC	Plasmin	Trypsin
29	500	1000	320	10,000	8000	>10,000
31	3200	160	80	10,000	2000	>10,000

fIIa = thrombin; tPA = tissue plasminogen activator; APC = activated protein C.

26. Phenylpyrrolidine TDI assays were carried out in house and expressed as fold decrease in enzyme activity after 30 min incubation. **31** did not demonstrate time-dependent inhibition of CYP1A2, CYP2C9, CYP2C19 or CYP2D6, or of CYP3A4 in the DEF assay, over a concentration range of 0.33–100 μM. However, it exhibited apparent time-dependent inhibition of CYP3A4 activity in the 7BQ assay with a 1.7-fold decrease at 33 μM (1.4× the IC_{50}) and 2.5-fold

at 100 μM (4× the IC_{50}).The observed decreases in activity should be compared with the 17-fold shift for **2** at 10 μM, its IC_{50}, in this assay.
27. The structure for **31** was refined at 1.69 Å (overall R_{merge} is 0.083) in Refmac5 to a final R_{factor} of 0.186 and R_{free} of 0.225 and **32** was refined at 2.19 Å (overall R_{merge} is 0.122) in Refmac5 to a final R_{factor} of 0.178 and R_{free} of 0.233 using procedures described in Ref. 4a. Coordinates are deposited in the protein data bank with codes 2y81 **31** and 2y82 **32**.
28. Bissantz, C.; Kuhn, B.; Stahl, M. *J. Med. Chem.* **2010**, *53*, 506.